

New antitumoral acetogenin ‘Guanacone type’ derivatives: Isolation and bioactivity. Molecular dynamics simulation of diacetyl-guanacone

Isabel Barrachina,^a Inmaculada Royo,^b Héctor A. Baldoni,^{c,d} Nadia Chahboune,^a Fernando Suvire,^c Nuria DePedro,^b M. Carmen Zafra-Polo,^a Almudena Bermejo,^{a,†} Noureddine El Aouad,^a Nuria Cabedo,^a Jairo Saez,^e José R. Tormo,^b Ricardo D. Enriz^c and Diego Cortes^{a,*}

^aDepartamento de Farmacología, Facultad de Farmacia, Universidad de Valencia, 46100 Burjassot, Valencia, Spain

^bCIBE-Merck Research Laboratories, Merck, Sharp & Dohme de ESPAÑA S.A., cl Josefa Valcárcel, 38, 28027 Madrid, Spain

^cDepartamento de Química, Universidad Nacional de San Luis, Chacabuco 915, 5700 San Luis, Argentina

^dInstituto de Matemática Aplicada San Luis (IMASL-CONICET), Ejército de los Andes 950, San Luis, Argentina

^eDepartamento de Química, Universidad de Antioquia, Medellín, Colombia

Received 12 December 2006; revised 12 April 2007; accepted 20 April 2007

Available online 25 April 2007

Abstract—We describe herein the isolation and semisynthesis of four acetogenin derivatives (**1–4**) as well as their ability to inhibit the mitochondrial respiratory chain and several tumor cell lines. In addition, four nanoseconds (ns) of MD simulation of compound **4**, in a fully hydrated POPC bilayer, is reported.

© 2007 Published by Elsevier Ltd.

1. Introduction

Annonaceous acetogenins (ACG) are bioactive plant secondary metabolites found only in several genera of the Annonaceae family. They are a unique class of long-chain fatty acid derivatives with potent in vivo and in vitro anticancer, pesticidal, and other biological effects. Most of the Annonaceous acetogenins contain a mono- or bis-tetrahydrofuran (THF) core and a terminal α , β -unsaturated γ -lactone ring (LR).^{1–5}

Guanacone (**1**) is a 10-keto bis-THF ACG isolated in 1998 from a cytotoxic organic extract of *Annona* aff. *spraguei* seeds.⁶ One of the nitrogenated semisynthetic guanacone derivatives was found to be a powerful inhibitor of mitochondrial complex I.^{6,7} Herein, we have examined the structure–activity relationships (SAR) of

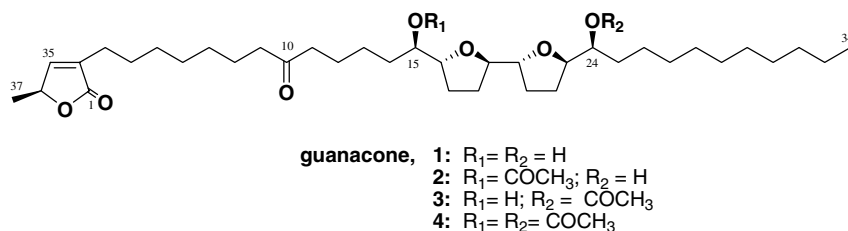
some natural and semisynthetic bis- and mono-THF ACG derivatives as growth inhibitors against several human tumor cell lines such as breast, lung, liver, and colon. The trends in the cytotoxicity assays were compared with the potency of the acetogenins as inhibitors of the mitochondrial respiratory chain.^{8–10}

The putative protein targets of ACG are the reduced nicotinamide-adenine dinucleotide NADH:ubiquinone oxidoreductase in complex I, which is a membrane-bound protein of the mitochondrial electron transport system,^{11,12} and the ubiquinone-linked NADH oxidase found in the plasma membrane of cancerous cells.¹³ A great number of studies have been performed in order to shed some light on the structural aspects and bioactivities of ACG and its congeners. However, the action mechanism of these compounds has received relatively little attention at least at molecular level. To date, accurate three-dimensional (3D) structural information for the ACG embedded in the membrane has not been available and the structural basis of ACG binding to the biological receptor is poorly understood. Guanacone derivatives (**1–4**) are lipophilic due to the long-chain fatty acid, being expected that they could be closely

Keywords: Annonaceae acetogenins; Molecular dynamics simulation; Tumor cell lines; Mitochondrial complex I.

* Corresponding author. Tel.: +34 963 54 49 75; fax: +34 963 54 49 43; e-mail: dcortes@uv.es

[†] Present address: Departamento de Citricultura, IVIA, crta Moncada-Náquera Km 4.5, 46113 Moncada, Valencia, Spain.



associated with the lipid membrane in which their enzyme targets reside. Membrane environment determines and limits the conformations and the location of lipophilic compounds acting at a membrane receptor in the lipid bilayer.^{14,15} Therefore, to determine the location and conformation of ACG in those membranes seems to be necessary to understand their role as potent cytotoxic compounds.

With the aim of comparing the SAR of these bis-THF ACG with a *threo/trans/threo/transerythro* relative configuration between their complex I and several tumor cell growth inhibition actions, we decided to test these four new natural or semisynthetic guanacone derivatives (1–4). In addition, we report here a Molecular dynamics (MD) simulation of diacetylguanacone (4) based on the Shimada model in presence of an explicit fully hydrated 1-palmitoyl-2-oleoyl-sn-glycero-3-phosphatidylcholine (POPC) bilayer, in order to shed light on some experimental data.^{14,15}

We describe herein the isolation and semisynthesis of four acetogenin derivatives (1–4) as well as their ability to inhibit the mitochondrial respiratory chain and several tumor cell lines. In addition, we have carried out a four nanoseconds (ns) of MD simulation of compound 4, in a fully hydrated POPC bilayer as reported.

2. Results and discussion

2.1. Isolation

Two new natural *O*-monoacetylated guanacone derivatives were isolated from the ethyl acetate extract of

Annona aff. *spraguei* (Annonaceae) seeds. 15-Acetylguanacone (2) and 24-acetylguanacone (3) were obtained after classic chromatographic purification and HPLC semipreparative partition with methanol/water/THF, 85:15:5. The molecular weight of 15-acetylguanacone (2) was determined by FABMS ion at m/z 662 $[M]^+$, corresponding to the molecular formula $C_{39}H_{66}O_8$. The presence of an α,β -unsaturated γ -lactone, an α,α' -dioxxygenated bis-THF system, and a keto group in 2 was deduced from the combined analysis of COSY 45, HSQC, and HMBC experiments (see Fig. 1). The existence in 2 of one hydroxyl and one acetoxy groups flanking the adjacent bis-tetrahydrofuran moiety was also confirmed by 2D NMR experiments. The location of the keto (position 10), acetoxy (position 15), and hydroxy (position 24) groups was confirmed by the fragments at m/z 223 and m/z 421 (see Fig. 1). 24-Acetylguanacone (3) is an isomer of 2 (see Fig. 2), which presents the keto, hydroxy, and acetoxy groups at 10, 15, and 24 positions, respectively. The relative stereochemistry across the α,α' -dioxxygenated bis-THF system of 2 and 3 was deduced as *threo/trans/threo/transerythro* based on their 1H and ^{13}C NMR data as well as on guanacone (1) and diacetylguanacone (4)⁶ structure (see Figs. 1 and 2).^{1,2,5}

2.2. Bioactivity

Table 1 shows the ED_{50} against the tumor cell lines and IC_{50} for inhibition of complex I of compounds 1–4. Similar to what had been observed in previous sets of *threo/trans/threo/transerythro* ACG,¹⁰ ED_{50} values were in the micromolar range, whereas IC_{50} values were in the nanomolar range. HepG2 (human liver carcinoma) was the most sensitive cell line to this set of ACG, followed by MCF-7 (breast), MES-SA (ovary), and MES-SA/Dx5

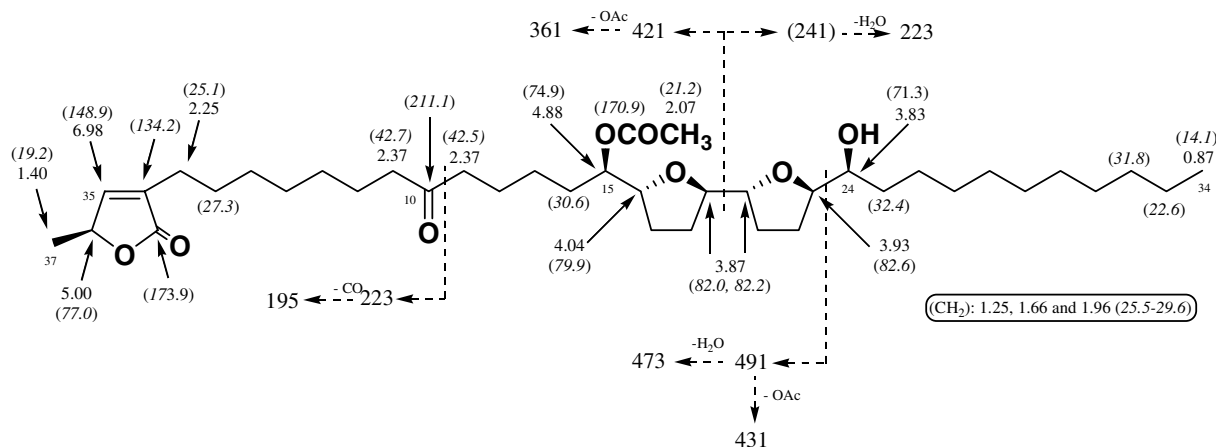


Figure 1. 1H NMR and ^{13}C NMR (in parentheses) spectral data and significant EIMS fragment ions of 15-acetylguanacone (2).

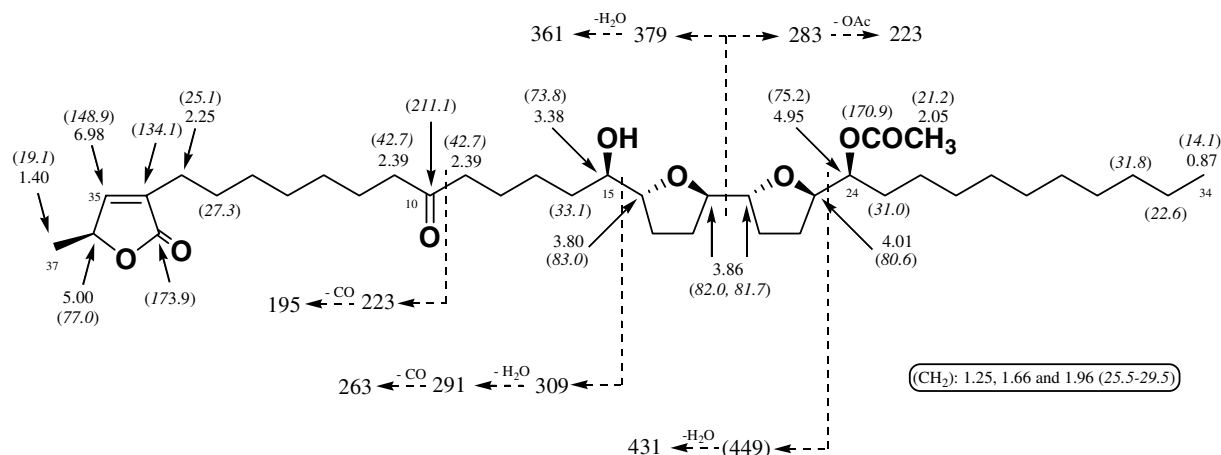


Figure 2. ¹H NMR and ¹³C NMR (in parentheses) spectral data and significant EIMS fragment ions of 24-acetylguanacone (3).

Table 1. Biological activity of the *threo/trans/threo/trans/erythro* bis-THF ACG studied with standard deviations

#	Compound	Max (μM)	ED ₅₀ ± SD (μM)						IC ₅₀ ± SD (nM)
			MCF-7	HepG2	vHT-29	A-549	MES-SA	MES-SA/Dx5	
1	Guacone ^a	250	39 ± 1	11 ± 1	71 ± 6	148 ± 3	22 ± 5	52 ± 8	1.2 ± 0.2
2	15-Acetyl-guacone	250	66 ± 17	51 ± 1	169 ± 24	101 ± 9	76 ± 12	97 ± 1	2.8 ± 0.4
3	24-Acetyl-guacone	250	50 ± 2	18 ± 1	154 ± 13	192 ± 15	43 ± 10	83 ± 3	3.4 ± 0.2
4	Di-acetyl-guacone	250	29 ± 6	9 ± 5	195 ± 11	60 ± 17	28 ± 7	56 ± 9	0.4 ± 0.1
5	Rotenone	500	161 ± 14	15 ± 6	202 ± 14	26 ± 7	147 ± 31	214 ± 41	5.1 ± 0.9
6	Doxorubicin	500	8 ± 3	102 ± 9	274 ± 19	152 ± 31	173 ± 54	>500 (40%)	—

Data shown are the ED₅₀ (Effective dose 50) observed for 50% inhibition of cell growth in the MTT cytotoxicity assay and the IC₅₀ (Inhibitory concentration 50) observed for NADH oxidase enzymatic inhibition. Max indicates the maximum concentration of the compound in the cytotoxicity assay titration.

^a Data from Refs. 7 and 10.

(ovary doxorubicin-resistant), being A-549 (lung) and HT-29 (colon) the less sensitive to these guanacone derivatives (1–4). Cytotoxicity against MES-SA cell line was slightly higher than the one observed against ovary doxorubicin resistant cell line (MES-SA/Dx5). These trends agreed with what had been previously observed for other *threo/trans/threo/trans/erythro* ACG.¹⁰ Whereas all these compounds were more active against the liver adenocarcinoma cell line. Diacetylguanacone (4) showed improved cell growth inhibition for MCF-7, HepG2, and A-549, whereas guanacone (1) was the most potent for the HT-29 cell line. In general these two ACG were the most potent of the series followed by the mono-acetyl derivatives, 2 and 3. Values observed for ED₅₀ were lower than the ones observed for *threo/trans/threo/trans/erythro* ACG.¹⁰ Oxo-, hydroxyl-, hydroxylimino-, *N*-acetyl, amino-, and *N*-formyl- analogs of guanacone had given ED₅₀ values one order of magnitude lower with the exception of 4 that resulted in the same range as other derivatives but with lower potency.¹⁰

Results for potency against mitochondrial complex I, measured as the inhibition of the integrated NADH oxidase enzymatic activity, agreed with the trends observed for inhibition of human tumor cell lines, being diacetylguanacone (4) one of the most potent of the *threo/trans/threo/trans/erythro* ACG described, with IC₅₀ val-

ues similar to the ones described for motrilin, deacetylvaricin, and 10-deoxo-10-hydroxyliminoguacone.^{6,7,10}

In these series, despite it being important that the steric impediments present at one or both sides of the bis-THF moiety due to the acetyl groups reduce their efficacy as cytotoxic or enzyme inhibition agents (natural ACG 2 and 3), the presence of two acetyl groups in 4 restored the potency to some extent. We had previously described that the keto groups along the alkyl chain at both sides of the bis-THF moiety seemed to enhance the interaction of these compounds with their target(s) inside the cell, what was observed for the 15,24-dioxoguacone derivative.¹⁰ This specificity trend seems to be present in the current guanacone-related compounds as diacetylguanacone (4), with two acetyl groups at the same positions of the two keto groups of 15,24-dioxoguacone, recovered or even improved the potency observed for 1 both in cell growth and enzymatic inhibition assays.

2.3. Molecular dynamics simulation

Despite a number of studies on their SAR in exerting biological effects,^{4–10} little is known about how ACG interact with the membrane bilayers. Differential scanning calorimetry (DSC) studies on dimyristoylphosphatidylcholine

(DMPC) with ACG dispersions showed that the ACG strongly interact at the hydrocarbon core/water interface of DMPC.¹⁵ In addition, ¹H NMR studies indicated that ACG have strong interactions between the protons of the THF rings of the ACG and those of the glycerol backbone of DMPC, as suggested by the DSC studies.¹⁴

Truncated NOE experiments¹⁵ pointed out that the THF rings of ACG reside near the polar interfacial head group region of the DMPC membrane lipids. This conclusion was also supported by the NOESY experiments in which the THF rings gave strong correlation with the

glycerol backbone region of DMPC. Shimada et al.^{14,15} reported that the THF rings with their flanking hydroxyl groups act as a hydrophilic anchor in the lipid membranes. The position of the THF ring anchor along the ACG chain determines the depth of the LR functional group, which then directly acts with the protein receptor site(s), perhaps mimicking the quinone ring of ubiquinone.^{16,17} The THF rings, acting as an anchor in the lipid bilayer, may thus enhance the bioactivity by restricting the location, conformation, and orientation of the functional LR moiety by interacting with the head group of the phospholipids.

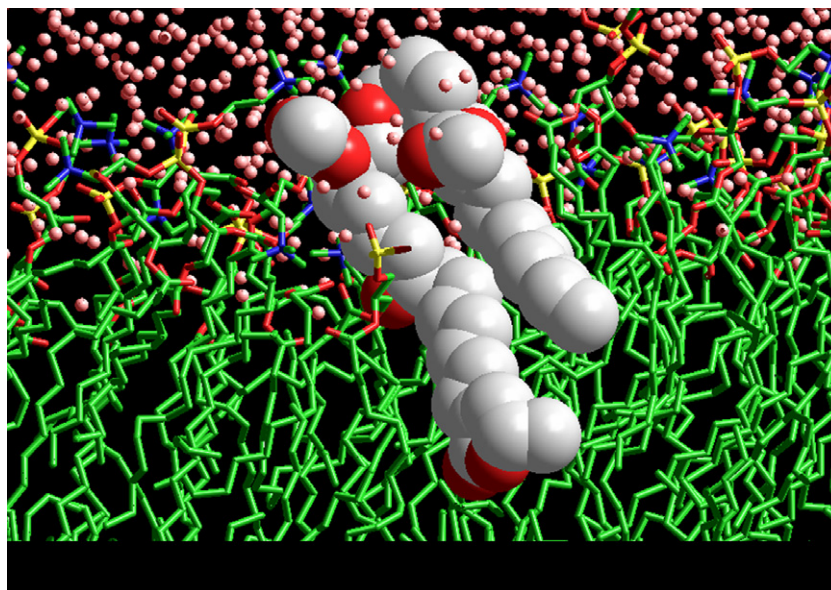


Figure 3. Snapshot of the diacetylguanacone (**4**) with the initial conformation ('hairpin' conformation) in the POPC bilayer. The molecules located ahead of the diacetylguanacone (**4**) as well as all the hydrogen atoms have been removed in order to facilitate the spatial view.

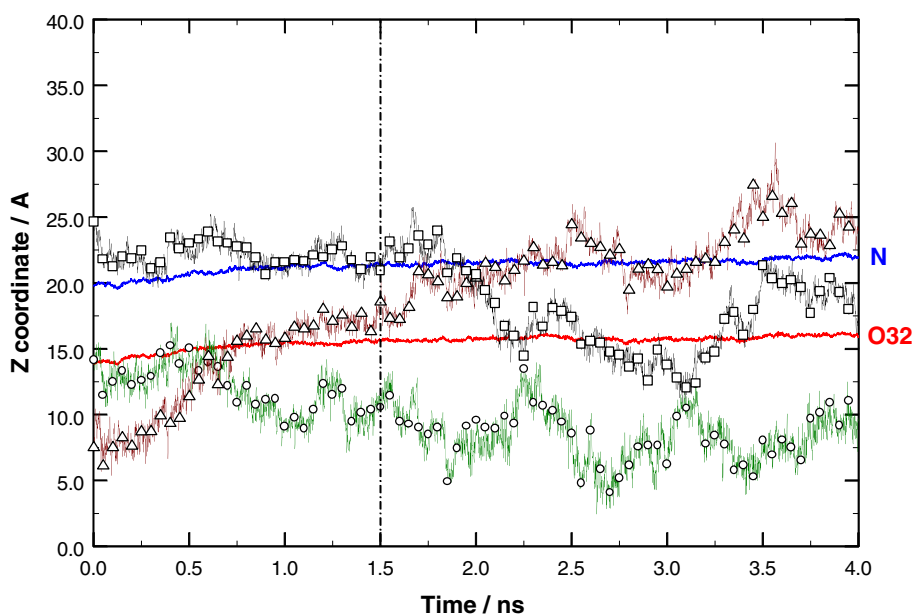
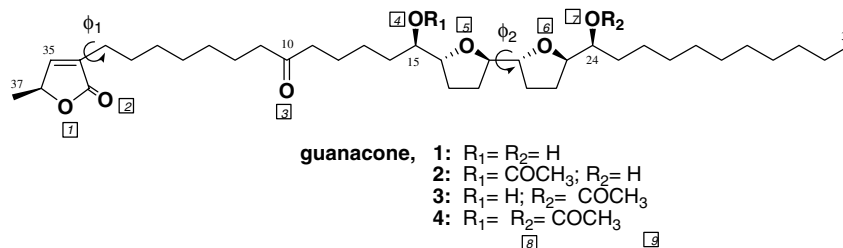


Figure 4. Time profiles along the membrane normal (z-coordinate) of the center of mass of the three diacetylguanacone (**4**) portions (○, -C34 of alkyl chain; △, THF and □, LR). The $Z = 0.0\text{Å}$ is the middle of the bilayer water phase. Horizontal lines labeled 'N' (in blue) and 'O32' (in red) indicate time average positions of the choline nitrogen atoms ($Z \sim 21.63 \pm 0.21\text{Å}$) and the carbonyl oxygen O32 atoms of glycerol ($Z \sim 15.80 \pm 0.18\text{Å}$), and indicate the width of the POPC/water interface.



Scheme 1. Conformation of guanacone derivatives.

On the basis of the above experimental data, in the present work, the conformation of diacetylguanacone (**4**) embedded into a POPC lipid bilayer was analyzed by determining the location of the THF, LR, and the alkyl chain portion. In addition, other dynamical parameters like orientations and conformations of the diacetylguanacone (**4**) system were analyzed in order to check up the model of Shimada et al.^{14,15}

2.4. Diacetylguanacone (**4**) in the POPC bilayer

2.4.1. Location of diacetylguanacone (4**).** In the initial step diacetylguanacone (**4**) molecule was placed in a bent ('hairpin') conformation in the POPC bilayer (Fig. 3).

After discarding the first 1.5 ns of trajectory, we have followed the changes of the location of the center of mass of three diacetylguanacone (**4**) portions (THF, LR, and the C34 of the alkyl chain). Figure 4 shows the location of the three different portions of diacetylguanacone (**4**) along the membrane normal (z -coordinate). In this figure, the labeled horizontal lines 'O32' and 'N' indicates the average position of the carbonyl oxygen O32 and the choline nitrogen atoms, respectively, and they represent the width of the POPC/water interface. During the production time (from ~ 1.5 to 4.0 ns) the C34 of the alkyl chain of diacetylguanacone (**4**) remained in the core region at 8.34 ± 2.0 Å from the bilayer center. In contrast the THF rings stayed in the POPC/water interface at 17.84 ± 3.14 Å from the bilayer center. From ~ 1.5 to ~ 3.0 ns of simulation, the LR moiety is located in the POPC/water interface. Whereas from ~ 3.0 to 4.0 ns this moiety reached the upper region of the POPC/water interface, as well as the bulk water at 23.73 ± 2.07 Å from the bilayer center. Figure 4 shows the overall simulation time (from 0.0 to 4.0 ns) in order to appreciate better the changes that take place during the simulation time. It should be noted that the LR in the starting 'hairpin' conformation was located relatively deeper into the hydrophobic core of the bilayer. The window time from 0.0 to ~ 1.5 ns shown in Figures 3 and 4 illustrates very well this situation.

2.4.2. Orientation and conformation of diacetylguanacone (4**).** In order to get meaningful information about the orientation of the diacetylguanacone (**4**) molecule from the simulation, the three virtual angles (α , β , and γ) were analyzed. We have defined two virtual intramolecular axes: (a) one linking the center of mass of the LR to the center of mass between C_{19} and C_{20} of the THF rings

(LR–T); and (b) linking the center of mass between C_{19} and C_{20} of the THF rings to the C_{34} atom (T– C_{34}) (see atom numbers in Scheme 1). From the previous defined axes we measured three angles: α (LR–T–Z), as the angle between the LR–T axis and the bilayer normal (z axis); β (T– C_{30} –Z), as the angle between the T– C_{34} axis and the bilayer normal (z axis); and γ (LR–T– C_{34}), as the intramolecular angle between axes LR–T and T– C_{34} . The γ angle is a measure of the hairpin opening. The analysis of the temporal evolution of the above virtual angles as a function of the time gives more insight into the orientation and the relationship between diacetylguanacone (**4**) conformation and the physical properties of the proposed active model for diacetylguanacone (**4**).¹⁴

From Figure 5a it is clear that the virtual angle α reaches over the last ~ 1.0 ns of simulation an average value of $87.16 \pm 8.89^\circ$. Whereas the virtual angle β , during the same period of time, takes an average value of $145.64 \pm 18.12^\circ$.

The γ angle changes in three steps: from 0.0 to ~ 1.0 ns takes a value close to 15° ; from ~ 1.0 to ~ 2.5 ns takes a value close to 60° and from ~ 2.5 to 4.0 ns adopts a value close to 90° (Fig. 5b).

Two main features can be inferred from the dependence of each virtual angle on time. On the one hand, transitions between orientations take place in a nanosecond time scale. On the other hand, it is remarkable that the γ angle, which represents the 'hairpin' opening, changes during the MD to an average value of $85.86 \pm 14.91^\circ$. These results indicate that diacetylguanacone (**4**) adopts a 'like-L' conformation.

In Figure 6, we show the evolution of the angles ϕ_1 and ϕ_2 (Scheme 1) with time. ϕ_1 , which represents the rotation of LR ring, displayed a significant flexibility ($-120.0 \leq \phi_1 \leq 120^\circ$). In contrast ϕ_2 , which represents the bond between both THF rings, oscillates around the mean value (-60°) without great changes; indicating a restricted rotation.

The above results indicated that diacetylguanacone (**4**) embedded in the POPC possesses a significant molecular flexibility and it was noted that this flexibility is a source of problem for precise NMR analysis either for the structural elucidation or for the conformational behavior of this molecule.

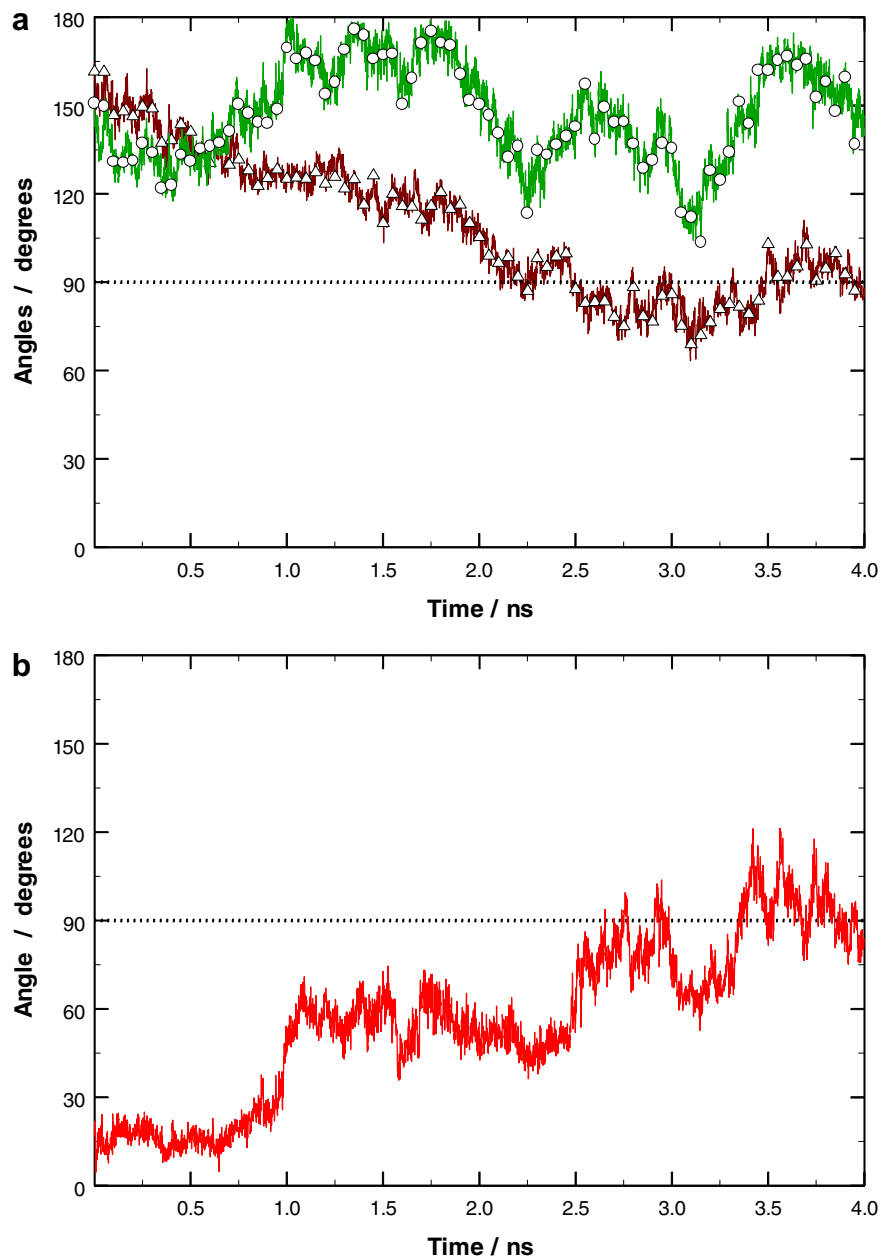


Figure 5. (a) Orientational angles α (Δ , LR) and β (\circ , $-\text{C34}$ of alkyl chain) with respect to the membrane normal as a function of the time; (b) time profile of the opening angle (γ) of the diacetylguanacone (**4**) hairpin conformation. The horizontal line (dot line) indicates an angle of 90° which corresponds to an orientation parallel to the membrane surface.

A snapshot of the location of diacetylguanacone (**4**) taken at ~ 3.6 ns of the simulation is shown in Figure 7a; the conformation adopted by diacetylguanacone (**4**) might be appreciated in this figure. Figure 7b, in turn, shows a snapshot of the diacetylguanacone (**4**)/POPC overall system at 3.6 ns of the MD simulation.

2.5. Hydrogen bond Interactions

In diacetylguanacone (**4**) there are basically six chemical groups containing oxygen atoms: sp^2 -hybridized carbonyl/carboxyl (O8 and O9), sp^2 -hybridized carbonyl/alkyl chain (O3), sp^2 -hybridized carbonyl/LR (O2), sp^3 -hybridized oxygen/THF (O5 and O6), sp^3 -hybrid-

ized carboxyl/ester (O4 and O7), and sp^3 -hybridized oxygen/LR (O1).

Table 2 gives the occupancies, lifetime, and geometrical parameters obtained for the different O atoms of diacetylguanacone (**4**) which are the potential proton-acceptors. MD simulations reveal that the principal occupancy occurs between the carbonyl/carboxyl O8 and the solvent with a lifetime of 1.8 ns over the last 2.5 ns. Also, significant percentages were obtained for the carbonyl/alkyl chain O3 (93.73% of occupancy and a lifetime of 2.0 ns) and the carbonyl/LR O2 showing 47.65% of occupancy and 1.9 ns of lifetime.

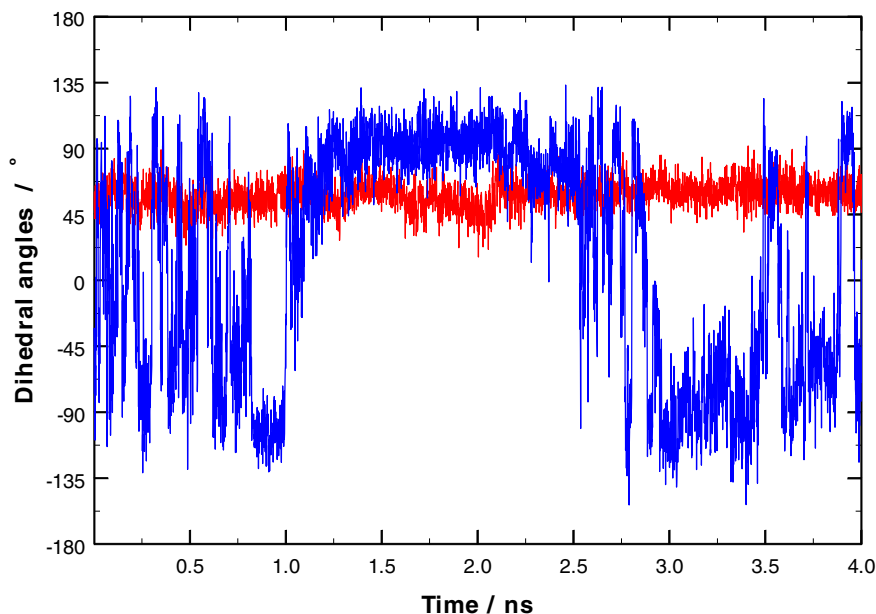


Figure 6. Temporal evolutions of dihedral angles Φ_1 and Φ_2 shown in Scheme 1.

2.5.1. DFT calculations. With the knowledge of the cardinal role of the electrostatic factors in the hydrogen bond interactions between the THF and the flanking acetyl groups of diacetylguanacone (**4**) with the solvent, Density Functional Theory (DFT) calculations were performed for a better understanding of the most representative H bond interactions at the sub-molecular level.

Model systems (see Table 3) were used to mimic the anchoring site of diacetylguanacone (**4**) and to enable quantum mechanical (QM) molecular orbital (MO) calculations. The use of model systems to simulate molecular interactions (MI) is necessary since diacetylguanacone (**4**) is too large for accurate DFT calculations. By using a model, one avoids dealing with complexities due to the rest of the diacetylguanacone (**4**) molecule. Thus, a better understanding of the inherent electronic properties of the active moieties of diacetylguanacone (**4**) reflected in the MI may be gained. When choosing a model system, the ability to reproduce electronic properties of the entire portion was considered. The energies of interaction (EI) were calculated with the approximation neglecting the superimposition of error due to the difference between the total energies of the complex with the sum of the total energies of the components:

$$EI = E_{Cx} - (E_{BC} - E_{AC})$$

Where EI is the energy interaction, E_{Cx} the complex energy, E_{BC} the energy of proton-donor component (i.e., Brønsted acid), and E_{AC} the energy of proton acceptor component (i.e., Brønsted base).

Table 3 gives the energies obtained for O8 (carbonyl/carboxyl)/water, O7 (carboxyl/ester)/water, O2 (THF)/water systems, and OH group/water (acting like donor and proton acceptor) from DFT calculations.

Although, for hydroxyl derivatives it would be necessary to determine the donor and/or acceptor character of each OH group, in the case of diacetylguanacone (**4**) this situation is simpler because the acetyl groups of diacetylguanacone (**4**) can act only as proton acceptors. From Table 3 it is clear that the most favored interaction occurs when the O8 (carbonyl/carboxyl) moiety is acting as acceptor, while the water molecule is the donor counterpart. The O2 (THF)/water system displays higher energy, while the O7 (carboxyl/ester)/water system has an intermediate value. Comparing the DFT calculations with the % occupied and lifetime parameters of Table 2 obtained from MD calculations, it is clear that both results are in a complete agreement.

We also performed DFT–MI calculations for the OH group acting like proton acceptor as well as proton donor (two last rows in Table 3). Our DFT results show that the complex with the oxygen atom acting as proton acceptor is energetically preferred by 6.44 kcal/mol at B3LYP/631G level and 2.91 at B3LYP/6-31++G (d,p) level with respect to the complex with the oxygen acting as proton donor.

It is interesting to note that DFT calculations predict that the molecular interactions between an OH group and water are lower but still comparable to that between the acetyl group and water. Thus, on the bases of these results it is reasonable to assume that the conformational behavior obtained for diacetylguanacone (**4**) could be closely related to those of hydroxyl derivatives or other acetogenins possessing the adequate polar groups.

3. Conclusions

All guanacone derivatives (**1–4**) assayed as growth inhibitors of human tumor breast, lung, liver, and colon

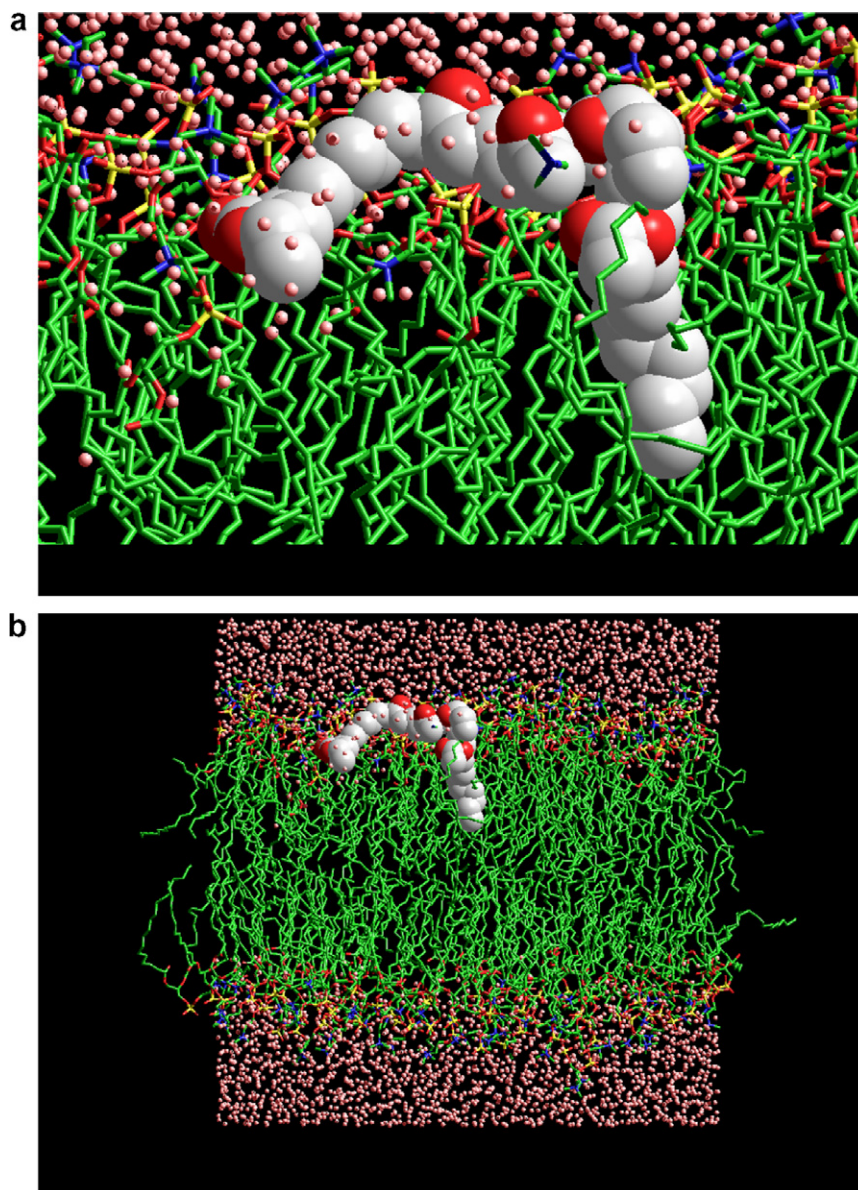


Figure 7. (a) Snapshot of the location of diacetylguanacone (**4**) taken at ~ 3.6 ns of the simulation. The conformation type ‘L’ adopted by diacetylguanacone (**4**) might be appreciated in this figure. (b) Snapshot of the diacetylguanacone (**4**)/POPC system at 3.6 ns of the MD simulation.

cell line, showed potencies in the micromolar range. These compounds showed potencies in the nanomolar range as inhibitors of mitochondrial respiratory chain.

A MD simulation of diacetylguanacone (**4**) in fully hydrated POPC lipid bilayer was performed. Thus, the MD trajectories of the guanacone–POPC bilayer complex were analyzed in order to provide a detailed dynamic model.

MD simulation revealed hydrogen bonds, which are critical to adopt a particular conformation, and indicated the important role of THF rings and the flanking acetyl groups for the geometry of this molecule. The resulting MD simulation plus molecular orbital calculations reproduced the hydrogen bonds constraining a putative ‘biologically relevant conformation’ of diacetylguanacone (**4**). LR and THF rings, located in the interface of the lipid bilayer, characterize this conforma-

tion. Our study emphasizes the role of the oxygen atoms of THF and particularly the flanking acetyl groups of diacetylguanacone (**4**) to form the hydrogen bond interactions, which stabilize this conformation with the solvent molecules. It must be pointed out that the results obtained for this compound might be extended to the rest of active acetogenins possessing flanking OH groups at the THF rings.

Results observed in this computer simulation, at least in part, were among the postulated mechanisms of ACG action.^{14,15} In this sense, the results reported here are in agreement with previously reported experimental findings. But the main advantage of MD simulations is that they describe in atomic level detail, the effect of a representative guanacone molecule on the phospholipid bilayer. This detail, often not available from observation, may be helpful in the interpretation of a large body of experimental data.

Table 2. Geometrical parameters, occupancies, and lifetime obtained for the different O atoms of diacetylguanacone (**4**) from MD calculations

Atom name ^a	Hydrogen bonds ^b			
	Length ^c (SD)	Angle ^d (SD)	Occupancy ^e	Lifetime ^f
Diacetylguanacone (4)				
O8	2.784 (0.12)	154.68 (13.44)	122.77	1.8
O3	2.779 (0.12)	156.26 (12.71)	93.73	2.0
O2	2.782 (0.12)	155.25 (13.39)	47.65	1.9
O9	2.800 (0.12)	155.79 (12.61)	29.85	2.0
O5	2.831 (0.11)	152.62 (14.16)	23.77	1.6
O1	2.838 (0.10)	148.88 (14.97)	10.42	1.9
O4	2.911 (0.06)	131.16 (7.37)	0.42	1.8
O7	2.856 (0.08)	139.77 (11.97)	0.31	2.0
O6	2.883 (0.03)	155.45 (7.20)	0.08	1.9
POPC				
O32	2.794 (0.12)	154.44 (13.37)	77.85	2.2

Note. The maximum perceptual occupancy for a given oxygen atom is 200% because it has two acceptor long pairs.

^a According to Scheme 1.

^b Calculated according to methods.

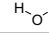
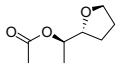
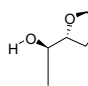
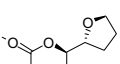
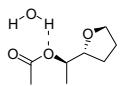
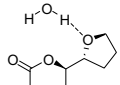
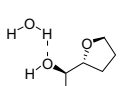
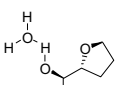
^c Å (standard deviation).

^d In degrees (standard deviation).

^e In percent.

^f In ns.

Table 3. The reduced models (denoted in the structure) interacting with water

		B3LYP/6-31G Energy (hartree)	B3LYP/6-31++G(d,p) Energy (hartree)
		-76.3861166	-76.433709
		-538.798889	-538.998948
Components		-386.186777	-386.333110
		-615.206248	-615.443991
		Interaction (Kcal/mol) 13.33	Interaction (Kcal/mol) 7.11
Complexes		-615.199659	-615.438419
		9.20	3.62
		-615.205387	-615.443508
		12.79	6.81
		-462.590162	-462.775098
		10.84	5.19
Complexes		-462.578292	-462.770457
		3.39	2.28

Energies (Hartree) obtained at two levels of theory for the complexes and components. Interaction energies (kcal/mol) obtained for the complexes are shown in bold.

We believe that the results presented in this paper could be regarded as a verification of some aspects of experimental data. However other results reported here are interesting complementary data for those experimental results. It is clear that the knowledge based on both approaches will increase our insight into the mechanism of diacetylguanacone (**4**) action in the lipid membranes.

4. Experimental

4.1. General experimental procedure

Optical rotations were determined on a Perkin-Elmer 241 polarimeter. IR spectra (film) were run on a Satellite FTIR-Mattson Serial 980514 spectrometer. MS (EIMS, FAB, and HREIMS) were determined on a VG Auto Spec Fisons spectrometer. Liquid chromatography with mass spectrometry detection (LC–MSD) with API source configured as API-ES in positive mode was carried out on a Hewlett–Packard HP-1100 Series. ¹H NMR (300 or 400 MHz) and ¹³C NMR (75 or 100 MHz) spectra were recorded on a Varian Unity-300 or a Varian Unity-400 instruments using the solvent signal as reference (CDCl₃ at δ 7.26 and 77.0). Multiplicities of ¹³C NMR resonances were assigned by DEPT experiments. COSY 45, HSQC, and HMBC correlations were run using a Varian Unity-400 MHz instrument. Chromatographic separations were carried out by column chromatography on silica gel 60H (5–40 μm, 7336 Merck) or by flash chromatography on silica gel 60 (230–400 μm, 9385 Merck) and semipreparative HPLC on a LiChroCartR 100 RP-18 column, using methanol/water/THF, 85:15:5.

4.2. Plant material

The seeds from *Annona* aff. *spraguei* Safford (Annonaceae), Colombian tree known as ‘guanacona’ or ‘tio-tio’, were collected from Sahagún town in Cordoba

region (Colombia). A voucher specimen was deposited, under Ref. 36732, at the National University of Medellin (Colombia).

4.3. Extraction and isolation

Dried, powdered seeds (1000 g) from *A. aff. spraguei* were defatted with petroleum ether. The defatted seeds were extracted with EtOAc and the concentrated extract (52 g) was partitioned between hexane and methanol. Five grams of the methanolic solution was subjected to column chromatography on silica gel 60H (CH₂Cl₂/EtOAc, 50:50), and then to semipreparative HPLC. Guanacone (**1**) (15 mg),⁶ 15-acetylguanacone (**2**) (6 mg), and 24-acetylguanacone (**3**) (4 mg) were isolated.

4.3.1. Guanacone (1). Amorphous powder; C₃₇H₆₄O₇; see Ref. 6.

4.3.2. 15-Acetylguanacone (2). Amorphous powder; C₃₉H₆₆O₈; [α]_D +12.5° (*c* 0.88, EtOH); IR, ν_{\max} (film) cm⁻¹ 3380, 2928, 2856, 1750, 1738, 1256, 749; FABMS *m/z* 662 [M]⁺; EIMSHR, *m/z* 491.2965 (calcd for C₂₈H₄₃O₇, 491.3008), 421.2574 (calcd for C₂₄H₃₇O₆, 421.2590), 223.1294 (calcd for C₁₃H₁₉O₃, 223.1334); EIMS, ¹H NMR and ¹³C NMR data see Figure 1.

4.3.3. 24-Acetylguanacone (3). Amorphous powder; C₃₉H₆₆O₈; [α]_D +10.3° (*c* 0.68, EtOH); IR, ν_{\max} (film) cm⁻¹ 3400, 2928, 2846, 1756, 1740, 1260, 749; FABMS *m/z* 662 [M]⁺; EIMSHR, *m/z* 431.2766 (calcd for C₂₆H₃₉O₅, 431.2797), 379.2549 (calcd for C₂₂H₃₅O₅, 379.2484), 309.2057 (calcd for C₁₈H₂₉O₄, 309.2066), 223.1311 (calcd for C₁₃H₁₉O₃, 223.1334); EIMS, ¹H NMR and ¹³C NMR data see Figure 2.

4.3.4. 15,24-Diacetylguanacone (4). Prepared from **1** (6 mg) by Ac₂O and pyridine at room temperature for 8 h, to obtain **4** in a quantitative yield; amorphous powder; C₄₁H₆₈O₉; see Ref. 6.

5. Bioassay experimental procedures

5.1. Enzyme inhibition

The inhibitory potency of the compounds was assayed using submitochondrial particles (SMP) from beef heart. SMP were obtained by extensive ultrasonic disruption of frozen-thawed mitochondria to produce open membrane fragments where permeability barriers to substrates were lost. Active complex I content in SMP preparations was estimated as previously described,¹⁸ giving a concentration of 45.8 ± 0.3 pmol mg⁻¹. SMP were diluted to 0.5 mg mL⁻¹ in 250 mM sucrose, 10 mM Tris-HCl buffer, pH 7.4, and treated with 300 μM NADH to activate complex I before starting experiments.

The enzymatic activities were assayed at 22 °C in 50 mM potassium phosphate buffer, pH 7.4, 1 mM EDTA with the SMP diluted to 6 μg mL⁻¹ (0.28 ± 0.01 nM complex I) in the cuvette. NADH oxidase activity was measured

as the aerobic oxidation of 75 μM NADH in the absence of external quinone substrates and other inhibitors of the respiratory chain. Reaction rates were calculated from the linear decrease of NADH concentration (λ = 340 nm, ϵ = 6.22 mM⁻¹ cm⁻¹) in an end-window photomultiplier spectrophotometer ATI-Unicam UV4-500.¹⁹

Stock solutions (2 mM in absolute ethanol) of the ACG used in this study were prepared and kept in the dark at -20 °C. Appropriate dilutions between 5 and 50 μM were made before the titrations. Increasing concentrations of these ethanolic solutions were then added to the diluted SMP preparations with 5-min incubation on ice between each addition. Maximal ethanol concentration never exceeded 2% of volume and control activity was not affected by this concentration.²⁰ After each addition of inhibitor the enzymatic activities involving complex I were measured as described. The inhibitory concentration 50 (IC₅₀) was taken as the final compound concentration in the assay medium that yielded 50% inhibition of either NADH oxidase activity. Given values are means ± SD of four assays for each compound.

5.2. Tumor cell lines

General growth and incubation conditions were the same as those in earlier experiments^{8–10} with six cell lines obtained from American Type Culture Collection (ATCC, Manassas, VA, USA). A-549 monolayer cells (human lung carcinoma, CCL-185) were maintained in Ham's F12 medium supplemented with 10% fetal bovine serum (FBS), 2 mM L-glutamine, 100 U mL⁻¹ penicillin, and 100 μg mL⁻¹ streptomycin. Hep-G2 cells (human liver carcinoma, CCL-8085) were grown in MEM with 10% qualified FBS, 2 mM L-glutamine, 1 mM sodium pyruvate, and 100 μM of MEM-non-essential-amino acids. MCF-7 cells (human breast HTB-22) were maintained in the previous medium supplemented with 0.01 mg mL⁻¹ bovine insulin, and HT-29 cells (human colon carcinoma HTB-38), MES-SA cells (human ovary carcinoma CRL-1976), and MES-SA/Dx5 monolayer cells (human ovary carcinoma doxorubicin-resistant CRL-1977) were cultured routinely in McCoy's 5A Medium modified with 10% FBS and 2 mM glutamine. All cell cultures were kept at 37 °C under a humidified atmosphere of 5% CO₂.

5.3. Antitumor assay

The general cytotoxic activity method used was similar to the one previously used for evaluating sets of bis-THF ACG^{8,10} and mono-THF ACG⁹ compounds. The MTT test was applied to the six cell lines for evaluation of the cytotoxic activity. The MTT test is an indirect measurement of cytotoxicity. It is based on the impaired ability of drug-treated cells to reduce the pale yellow MTT to a deep blue formazan. NADH is provided directly by the cells which in turn require proper metabolic function. Therefore, inhibition of the MTT reduction rate is an indicator of the functional integrity of the mitochondria and, hence, of cellular viability.²¹ Samples (10 μl) were incubated with 60–80% of confluent culture

of each cell line for 24 h in an atmosphere of 5% CO₂ at 37 °C. The titration range started at the concentrations indicated in Table 1. Each compound was titrated in twofold serial dilutions per triplicate. Absorption at 490 nm was measured in a Victor2™ Wallac spectrofluorometer. Effective dose 50 (ED₅₀) was determined as the inhibitor concentration that killed 50% of tumor cells. Actinomycin D and doxorubicin were used as controls.

6. Calculation methods

6.1. Molecular dynamic environment

We chose 1-palmitoyl-2-oleoyl-sn-glycero-3-phosphatidylcholine (POPC) as the lipid molecule and TIP3P as the water model²². POPC was chosen as the lipid molecule because it is the most common class of phosphatidylcholine lipid in biological membranes. Also this lipid contains an unsaturated carbon–carbon bond in one of its tails (i.e., P16:0/O18:1) making it a better choice for modeling biological membranes than lipids with only saturated tails.

A pre-equilibrated and well-characterized structure of a POPC bilayer in the liquid–crystal phase was available to model the starting lipid structure.²³ Insertion of the diacetylguanacone (**4**) into the lipid bilayer, minimization of the starting structure, and equilibration are described in detail as follows.

6.2. System setup

A bilayer of 200 1-palmitoyl-2-oleoyl-sn-glycero-3-phosphatidylcholine lipid covered with water on the intra- and extracellular sides was used as starting structure for the diacetylguanacone (**4**) environment.²³ For all MD simulations, energy minimization, and structural analysis the AMBER 7 program was used.²⁴ The generalized amber force field²⁵ was applied to all the atoms in the system in the full atomic detail. Atomic partial charges for POPC were taken from previous reports,^{26,27} whereas atomic partial charges for diacetylguanacone (**4**) were those obtained by antechamber at the AM1-BCC procedure.²⁸ Water molecules were based on the TIP3P model.²²

To overcome severe van der Waals repulsion between POPC bilayer and diacetylguanacone (**4**) this compound was placed in a hole created after deletion of a single lipid in the original membrane³³ in a ‘hairpin’ conformation as was previously obtained.²⁹ In the starting conformation the THF rings of diacetylguanacone (**4**) were placed at the interface region of the lipid bilayer, whereas the hydrophobic tail and the α,β -unsaturated system were placed in the hydrophobic core of the lipid bilayer as shown in Figure 3. Finally the system consists of 199 POPC, one diacetylguanacone (**4**), and 5600 TIP3P water molecules. The ratio of water to lipid molecules (n_w) was ~ 28 allowing a proper hydration of the lipid bilayer.³⁰ The size of the system was 43,584 total atoms.

The simulation box was rotated in such a way that the phosphatidylcholine (PC) head groups of POPC were placed in the xy -plane of the interface and the z -axis was parallel to the membrane normal. After that, the box center of mass was moved to the geometrical center of the orthogonal system. Due to the charge of the system being zero no counterions were needed to electro-neutralize the system.

Analysis of H bonds was performed with the ptraj module of the AMBER package. Percentual occupancies and lifetime were calculated as the function of the time that an H bond between proton water (Hw) atoms and the corresponding diacetylguanacone (**4**) oxygens is formed. In the analysis, H bonds were considered to be formed when the distance cutoff between heavy atoms of a donor and an acceptor was ≤ 3.0 Å and the donor-H-acceptor angle $> 120.0^\circ$. Hydrogen bonds were dumped for occupancies $> 0.0\%$ and evaluated during the last 2.5 ns of the MD simulation.

6.3. Equilibration conditions

MD simulation was carried out on the systems formed by POPC/water/diacetylguanacone (**4**) for 4.0 ns and the following procedure was applied:

First of all a steepest descent minimization was run during 1000 cycles to reach the initial configuration to relax bad van der Waals contacts, bringing the system to a local minimum. The diacetylguanacone (**4**) was held in place by a harmonic potential constraint of $500 \text{ kcal mol}^{-1} \text{ \AA}^{-1}$, whereas the rest of the system (i.e., POPC/water) was freely allowed to move. Following the constrained minimization a constrained equilibration at the constant volume–temperature (NVT) ensemble was started during 385 picoseconds (ps) applying a harmonic potential constraint of $500 \text{ kcal mol}^{-1} \text{ \AA}^{-1}$ to the diacetylguanacone (**4**). During the first 10 ps the system was slowly heated from 0 to 37 °C. After that the system was allowed to evolve another 375 ps.

After the NVT equilibration, isobaric-isothermal (NPT) ensemble was performed during 115 ps in two stages. During the first 20 ps a harmonic potential constraint of $500 \text{ kcal mol}^{-1} \text{ \AA}^{-1}$ to the diacetylguanacone (**4**) was applied. After that all constraints were switched off and the system was run during 95 ps to round 500 ps of equilibration. From this point on throughout the rest of the simulation (4.0 ns) the system was kept at the NPT ensemble.

The last 2.5 ns were considered as the production part of the simulation. Energies and coordinates were written after each picosecond to the subsequent analysis. Other simulation conditions were the following: electrostatic interactions within the MD simulation were calculated using the PME method.³¹ The cutoff for the Lennard-Jones interactions was 8 Å and bonds between hydrogen and heavy atoms were constrained with the SHAKE algorithm³² permitting the use of 2 fs time steps to integrate the equations of motion.

The temperature was kept close to ~ 310 K (~ 37 °C), which is above the main phase transition temperature for a POPC bilayer (-5 °C),³³ using a Berendsen thermostat.³⁴ Pressure was controlled by a Berendsen barostat.³⁴ Pressure coupling was applied anisotropically, each direction being treated independently with the trace of the pressure tensor kept constant to 1 atm.

To avoid the ‘cold solute/hot solvent’ problem velocity reassignments to the target temperature in conjunction with the removal of the system center of mass motion were applied at every 1 ps as was suggested previously.³⁵ Others control parameters were left as its default values.

The Hyperchem program was used as the graphic interface to visualize the diacetylguanacone (**4**)/POPC system.³⁶

6.3.1. DFT calculations. For the molecular interaction (MI) calculations, all the complexes under investigation were initially optimized using B3LYP/6-31G(d) level of theory. Correlation effects were included using Density Functional Theory (DFT) with the Becke 3–Lee–Yang–Parr (B3LYP)³⁷ functional and the 6-31++G(d,p) basis set for all the complexes obtained at the lower level of computation. During the B3LYP/6-31++G(d,p) calculations, the B3LYP/6-31G(d) geometries were kept fixed. These calculations were carried out using the Gaussian 03 program.³⁸

Acknowledgments

This research was supported by the Spanish Dirección General de Investigación (Grant SAF 2001-3142). We also thank the Conselleria d'Empresa, Universitat i Ciència de la Generalitat Valenciana for the Grant GRUPOS 05/038. The continuous financial support from the Universidad Nacional de San Luis is gratefully acknowledged. H.A.B. and R.D.E. are members of the scientific staff of CONICET (Argentina). H.A.B. is grateful to acknowledge Dr. David A. Case (The Scripps Research Institute) for providing him access to Amber 7 suite of programs, as well as Ing. Marta B. Caldentey (Supercomputing Center of Buenos Aires, SeCyT, Argentina) for technical support. Calculations were performed on a 40 processors SGI Origin2000 at the Supercomputing Center of Buenos Aires (SeCyT, Argentina).

Supplementary data

Supplementary data associated with this article can be found, in the online version, at doi:10.1016/j.bmc.2007.04.039.

References and notes

- Cavé, A.; Figadère, B.; Laurens, A.; Cortes, D. Acetogenins from Annonaceae. In *Progress in the Chemistry of Organic Natural Products*; Herz, W., Kirby, G. W., Moore, R. E., Steglich, W., Tamm, Ch., Eds.; Springer: New York, 1997; Vol. 70, pp 81–288.
- Zafra-Polo, M. C.; Figadère, B.; Gallardo, T.; Tormo, J. R.; Cortes, D. *Phytochemistry* **1998**, *48*, 1087–1117.
- Alali, F. Q.; Liu, X. X.; McLaughlin, J. L. *J. Nat. Prod.* **1999**, *62*, 504–540.
- Tormo, J. R.; Gallardo, T.; González, M. C.; Bermejo, A.; Cabedo, N.; Andreu, I.; Estornell, E. *Curr. Topics Phytochem.* **1999**, *2*, 69–90.
- Bermejo, A.; Figadère, B.; Zafra-Polo, M. C.; Barrachina, I.; Estornell, E.; Cortes, D. *Nat. Prod. Rep.* **2005**, *22*, 269–303.
- Gallardo, T.; Sáez, J.; Granados, H.; Tormo, J. R.; Vélez, I. D.; Brun, N.; Torres, B.; Cortes, D. *J. Nat. Prod.* **1998**, *61*, 1001–1005.
- Gallardo, T.; Zafra-Polo, M. C.; Tormo, J. R.; González, M. C.; Franck, X.; Estornell, E.; Cortes, D. *J. Med. Chem.* **2000**, *43*, 4793–4800.
- Royo, I.; DePedro, N.; Estornell, E.; Cortes, D.; Pélaez, F.; Tormo, J. R. *Oncol. Res.* **2003**, *13*, 521–528.
- Tormo, J. R.; Royo, I.; Gallardo, T.; Zafra-Polo, M. C.; Hernández, P.; Cortes, D.; Pélaez, F. *Oncol. Res.* **2003**, *14*, 147–154.
- Tormo, J. R.; DePedro, N.; Royo, I.; Barrachina, I.; Zafra-Polo, M. C.; Cuadrillero, C.; Hernández, P.; Cortes, D.; Pélaez, F. *Oncol. Res.* **2005**, *15*, 129–138.
- Ahmadshah, K. I.; Hollingworth, R. M.; McGovern, J. P.; Hui, Y. H.; McLaughlin, J. L. *Life Sci.* **1993**, *53*, 1113–1120.
- Friedrich, T.; Van Heek, P.; Leif, H.; Ohnishi, T.; Forche, E.; Kunze, B.; Jansen, R.; Trowitzsch-Kienast, W.; Hofle, G.; Reichenbach, H.; Weiss, H. *Eur. J. Biochem.* **1994**, *219*, 691–698.
- Morré, J. D.; DeCabo, R.; Farley, C.; Oberlies, N. H.; McLaughlin, J. L. *Life Sci.* **1995**, *56*, 343–348.
- Shimada, H.; Kozlowski, J. F.; McLaughlin, J. L. *Pharmacol. Res.* **1998**, *37*, 357–363.
- Shimada, H.; Grutznier, J. B.; Kozlowski, J. F.; McLaughlin, J. L. *Biochemistry* **1998**, *37*, 854–866.
- Metz, G.; Howard, K. P.; Van Liemt, W. B. S.; Prestegard, J. H.; Lugtenburg, J.; Smith, S. O. *J. Am. Chem. Soc.* **1995**, *117*, 564–565.
- Miyoshi, H.; Inoue, M.; Okamoto, S.; Ohshima, M.; Sakamoto, K.; Iwamura, H. *J. Biol. Chem.* **1997**, *272*, 16176–16183.
- Fato, R.; Estornell, E.; Di Bernardo, S.; Pallotti, F.; Parenti-Castelli, G.; Lenaz, G. *Biochemistry* **1996**, *35*, 2705–2716.
- Estornell, E.; Fato, R.; Pallotti, F.; Lenaz, G. *FEBS Lett.* **1993**, *332*, 127–131.
- Degli Esposti, M.; Ghelli, A.; Ratta, M.; Cortes, D.; Estornell, E. *Biochem. J.* **1994**, *301*, 161–167.
- Corine, V.; Coiffard, C.; Coiffard, L. J. M.; Rivalland, P.; De Roeck-Holtzhauer, Y. *J. Pharmacol. Toxicol.* **1998**, *39*, 143–146.
- Jorgensen, W. L.; Chandrasekhar, J.; Madura, J. D.; Impey, R. W.; Klein, M. L. *J. Chem. Phys.* **1983**, *79*, 926–935.
- Heller, H.; Schaefer, M.; Schulten, K. *J. Phys. Chem.* **1993**, *97*, 8343–8360.
- Case, D. A.; Pearlman, D. A.; Caldwell, J. W.; Cheatham III, T. E.; Wang, J.; Ross, W. S.; Simmerling, C. L.; Darden, T. A.; Merz, K. M.; Stanton, R. V.; Cheng, A. L.; Vincent, J. J.; Crowley, M.; Tsui, V.; Gohlke, H.; Radmer, R. J.; Duan, Y.; Pitera, J.; Massova, I.; Seibel, G. L.; Singh, U. C.; Weiner, P. K.; Kollman, P. A.; **2002**, AMBER 7, University of California, San Francisco.
- Wang, J.; Wolf, R. M.; Caldwell, J. W.; Kollman, P. A.; Case, D. A. *J. Comput. Chem.* **2004**, *25*, 1157–1174.
- Schlenkrich, M.; Brickmann, J.; MacKerell, A. D., Jr.; Karplus, M. An empirical potential energy function for

- phospholipids: criteria for parameter optimization and applications In *Biological Membranes: A Molecular Perspective from Computation and Experiment*; Merz, K. M., Roux, B., Eds.; Birkhauser: Boston, 1996; pp 31–82.
27. Feller, S. E.; MacKerell, A. D., Jr. *J. Phys. Chem. B* **2000**, *104*, 7510–7515.
28. Jakalian, A.; Bush, B. L.; Jack, D. B.; Bayly, C. I. *J. Comput. Chem.* **2000**, *21*, 132–146; Jakalian, A.; Jack, D. B.; Bayly, C. I. *J. Comput. Chem.* **2002**, *23*, 1623–1641.
29. Suvire, F. D.; Baldoni, H. A.; Bombasaro, J. A.; Enriz, R. D. Simulación de las interacciones de solvatación de los grupos polares de guanacina y derivados, en su sitio de anclaje *1er. Workshop Argentino de Química Medicinal, Buenos Aires 26 y 27 de Mayo de 2005*, pp 25–26.
30. Petrache, H. I.; Feller, S. E.; Nagle, J. F. *Biophys. J.* **1997**, *72*, 2237–2242.
31. Essmann, U.; Perera, L.; Berkowitz, M. L.; Darden, T.; Lee, H.; Pedersen, L. G. *J. Chem. Phys.* **1995**, *103*, 8577–8593.
32. Ryckaert, J.-P.; Ciccoliti, G.; Berendsen, H. J. C. *J. Comput. Phys.* **1977**, *23*, 327–341.
33. Seelig, J.; Waespe-Sarcevic, N. *Biochemistry* **1978**, *17*, 3310–3315.
34. Berendsen, H. J. C.; Postma, J. P. M.; Van Gunsteren, W. F.; Di Nola, D.; Haak, J. R. *J. Chem. Phys.* **1984**, *81*, 3684–3690.
35. Harvey, S. C.; Tan, R. K. Z.; Cheatham, T. E., III *J. Comput. Chem.* **1998**, *19*, 726–740.
36. HYPERCHEM. Release 5 for Windows. Hypercube Inc. **1998**.
37. Becke, A. D. *Phys. Rev. A* **1998**, *38*, 3098–3100; Becke, A. D. *J. Chem. Phys.* **1993**, *98*, 5618–5652; Lee, C.; Yang, W.; Parr, R. G. *Phys. Rev. B* **1998**, *37*, 785–789.
38. Frisch, M. J.; Trucks, G. W.; Schlegel, H. B.; Scuseria, G. E.; Robb, M. A.; Cheeseman, J. R.; Montgomery, J. A. Jr.; Vreven, T.; Kudin, K. N.; Burant, J. C.; Millam, J. M.; Iyengar, S. S.; Tomasi, J.; Barone, V.; Mennucci, B.; Cossi, M.; Scalmani, G.; Rega, N.; Petersson, G. A.; Nakatsuji, H.; Hada, M.; Ehara, M.; Toyota, K.; Fukuda, R.; Hasegawa, J.; Ishida, M.; Nakajima, T.; Honda, Y.; Kitao, O.; Nakai, H.; Klene, M.; Li, X.; Knox, J. E.; Hratchian, H. P.; Cross, J. B.; Adamo, C.; Jaramillo, J.; Gomperts, R.; Stratmann, R. E.; Yazyev, O.; Austin, A. J.; Cammi, R.; Pomelli, C.; Ochterski, J. W.; Ayala, P. Y.; Morokuma, K.; Voth, G. A.; Salvador, P.; Dannenberg, J. J.; Zakrzewski, V. G.; Dapprich, S.; Daniels, A. D.; Strain, M. C.; Farkas, O.; Malick, D. K.; Rabuck, A. D.; Raghavachari, K.; Foresman, J. B.; Ortiz, J. V.; Cui, Q.; Baboul, A. G.; Clifford, S.; Cioslowski, J.; Stefanov, B. B.; Liu, G.; Liashenko, A.; Piskorz, P.; Komaromi, I.; Martin, R. L.; Fox, D. J.; Keith, T.; Al-Laham, M. A.; Peng, C. Y.; Nanayakkara, A.; Challacombe, M.; Gill, P. M. W.; Johnson, B.; Chen, W.; Wong, M. W.; Gonzalez, C.; Pople, J. A. Gaussian 03, Revision B.05 **2003**, Gaussian, Inc., Pittsburgh PA.